

Excited QCD, Zakopane, 13th February 2009

## The nature of the $X(2175)$

Susana Coito

CFIF, Instituto Superior Técnico, Lisboa

Collaboration with: George Rupp, Eef van Beveren

- I. The  $X(2175)$
- II. The Resonance Spectrum Expansion Model and the  $X(2175)$
- III. Finding and following poles
- IV. Conclusions and improvements

## I. The $X(2175)$ or $Y(2175)$ or $\phi(2170)$

- Detected by BABAR (in 2006) in the production process  $e^+e^- \rightarrow \phi(1020)f_0(980)$  and it was identified as a  $1^{--}$  resonance with:

$$m = 2.175 \pm 0.010 \pm 0.015 \text{ GeV}, \Gamma = 58 \pm 16 \pm 20 \text{ MeV}$$

- Also discovered by BES in  $J\psi \rightarrow \eta\phi f_0(980)$  with:

$$m = 2.186 \pm 0.010 \pm 0.006 \text{ GeV}, \Gamma = 65 \pm 25 \pm 17 \text{ MeV}$$

- And now in PDG (2008).

– > Torres et al. (PRD 78 (2008) 074031) - Faddeev calculation for three mesons  $\phi K \bar{K}$

$$2110 \sim 2150 \text{ MeV}, \Gamma = 27 \text{ MeV}$$

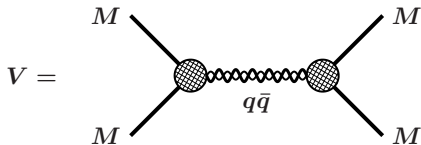
– > Napsuciale et al. (PRD 76 (2007) 074012) - Conventional  $R\chi PT$  calculation cannot reproduce the peak, giving rise to some speculation about its possible exotic character.

Exotic approaches usually find too large widths.

## II. The Resonance Spectrum Expansion Model ...

In this model we treat elastic-scattering processes of the form  $AB \rightarrow CD$ , where  $A, B, C$  and  $D$  are non-exotic mesons. In the present work, we consider only meson states composed of  $u, d$  and  $s$  quarks.

This idea can be represented by the following diagram:



We see we have two phases, one in which we have several two-meson states and another in which we have a whole spectrum of simple  $q\bar{q}$  states. The mechanism for the transition is the annihilation of a quark pair at the first vertex and the creation of another quark pair at the second vertex, according to the OZI rule.

We define an effective potential for this picture, given in momentum space, by:

$$V_{ij}(p_i, p'_j; E) = \lambda^2 j_{L_i}^i(p_i a) j_{L_j}^j(p'_j a) \sum_{n=0}^{\infty} \frac{g_i(n) g_j(n)}{E - E_n}$$

Here we have taken spherical delta function for the transition potential, which becomes a spherical Bessel function in momentum space.

We have two free parameters with physical meaning:

$a$  - interaction distance for the transition

$\lambda$  - global coupling

The dynamical part of the potential is given by a sum over the whole confinement spectrum (each  $E_n$  is an eigenvalue of this spectrum), which explains the model's name - Resonance Spectrum Expansion (RSE).

Now we write the coupled-channel Lippmann-Schwinger (LS) equation for the transition matrix:

$$T_{ij}(p_i, p'_j; E) = V_{ij}(p_i, p'_j; E) + \sum_m \int dk k^2 V_{im}(p_i, p'_m; E) G_0^{(m)}(k; E) T_{mj}(k, p'_j; E)$$

The Green's function is a diagonal matrix given by:

$$G_0^{(m)} = \left( E - \frac{k^2}{2\mu_m} - i\epsilon \right)^{-1}$$

As our potential is separable, we can evaluate the LS equation in closed form. It just amounts to summing up all  $s$ -channel meson loops.

The loop function for meson-meson channel  $m$  can be easily evaluated as:

$$\Omega^{(m)} = -i2aj_{L_m}(p_m a) h_{L_m}^{(1)}(p_m a) p_m \mu_m$$

Note that we shall use relativistic momenta and reduced masses henceforth.

Let us now return to the RSE formula:

$$R_{ij}(E) = \lambda^2 \sum_{n=0}^{\infty} \frac{g_i(n)g_j(n)}{E - E_n}$$

Besides the global coupling parameter  $\lambda$  we have, in this equation many coupling constants  $g_i(n)$ , corresponding to the couplings of all RSE states to all decay channels. These constants have been evaluated by Eef van Beveren, using expansions on a harmonic-oscillator (HO) basis for the  $^3P_0$  model, and decreases very rapidly as the radial quantum number  $n$  increases.

In practice, we consider the first 20 terms of the expansion, which is more than sufficient for convergence of the series.

Finally, we choose a confinement potential, taking the harmonic oscillator, for simplicity, but also because it works in phenomenological applications. The well-known spectrum reads:

$$E_n = m_q + m_{\bar{q}} + \omega(2n + 3/2 + L)$$

The use of this potential is not strictly necessary, but it is very convenient for this first study.

Also, an important property of the model is the manifest unitarity of the scattering matrix, whose relation to the transition matrix is given by:

$$S = \mathbb{1} + 2iT$$

## II. ...and the $X(2175)$

We treat our particle as a  $\phi$  state ( $1^{--}$ ) with a pure  $s\bar{s}$  configuration and, for simplicity, only the  ${}^3S_1$  component.

Table: HO eigenvalues in GeV with  $\omega = 0.19$  and  $L = 0$

$n$	$s\bar{s}$
0	1.301
1	1.681
2	2.061
3	2.441
4	2.821



Table: Thresholds of included meson-meson channels, in GeV

Channel	relative L,S	Threshold
$KK$	1, 0	0.987
$KK^*$	1, 1	1.388
$\eta\phi$	1, 1	1.567
$\eta'\phi$	1, 1	1.977
$K^*K^*$	1, 0	1.788
$K^*K^*$	1, 2	1.788
$f_0\phi$	0, 1	1.999
$\kappa K^*$	0, 1	1.639
$\eta h_1(1380)$	0, 1	1.928
$\eta' h_1(1380)$	0, 1	2.338
$KK_1(1270)$	0, 1	1.764
$KK_1(1400)$	0, 1	1.894
$K^*K_1(1270)$	0, 1	2.164
$K^*K_1(1400)$	0, 1	2.294
$\phi f_1(1420)$	0, 1	2.439

### III. Finding and following poles

After programming the transition matrix, we need to adjust our two free parameters.

We start by searching the known  $\phi(1020)$  pole in the 2nd Riemann sheet.

For  $\mathbf{a} = \mathbf{5.0} \text{ GeV}^{-1}$  and  $\mathbf{\lambda} = \mathbf{3.75} \text{ GeV}^{-3/2}$  we find:

$$1.0151 - i0.0035 \text{ GeV}$$

Compared with the PDG value:

$$1.0195 - i0.0021$$

Although the width is a bit large, we consider it a reasonable approximation, for the purpose of this study.

Now we introduce an artificial new parameter,  $\beta$ , which allows to continuously turn on and off all channels except for the most relevant one in the energy region of concern. It may be varied between 0 and 1.

For  $\beta = 0.0$ , we have in practice only one decay channel.

For  $\beta = 1.0$ , all channels contribute fully.

In the case of the  $\phi(1020)$ , the most important channel is  $KK$ . Switching off all other channels ( $\beta = 0.0$ ), we find the pole at:

$$1.144 - i0.065 \text{ GeV}$$

$\therefore$  Increasing  $\beta$  from 0 to 1 then makes the other (closed) channels move the pole to smaller values of its real part, in the direction of the  $KK$  threshold. The final pole position is, of course, the value found before (previous slide).

With the parameter values  $a$  and  $\lambda$  fixed before, we now explore the energy region above 2.0 GeV. We find the following poles (all channels included):

$$\begin{aligned}2.260 - i0.094 &- > \text{continuum pole} \\2.596 - i0.118 &- > \text{continuum pole} \\1.966 - i0.026 &- > \text{confinement pole } n = 2 \\2.367 - i0.051 &- > \text{confinement pole } n = 3 \\2.789 - i0.036 &- > \text{confinement pole } n = 4\end{aligned}$$

To find out whether a pole is dynamically generated or comes from the confinement spectrum, we follow them in the complex plane by reducing the  $\lambda$  value.

Now we choose the  $f_0(980)\phi$  channel as the relevant one and decouple all others ( $\beta = 0$ ). Then, the first continuum pole comes out at  $2.190 - i0.070$ , not far from the  $X(2175)$ .

Turning on the other channels, it seems the pole moves far away but then turns back (see figure), so no definite conclusion can be drawn. A more detailed investigation is needed, because the coupled-channel effects are very large. In the next three figures, we show some pole trajectories as a function of  $\lambda$ .

Figure: 1st Continuum pole's motion by changing  $\beta$

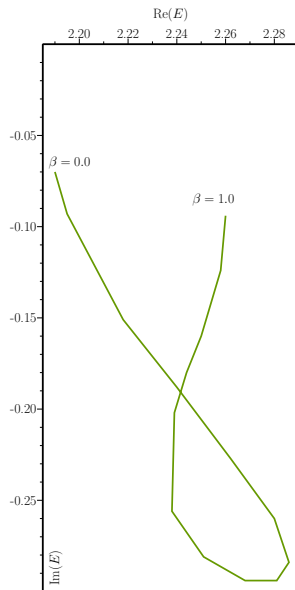


Figure: 1st Continuum pole's motion by changing  $\lambda$

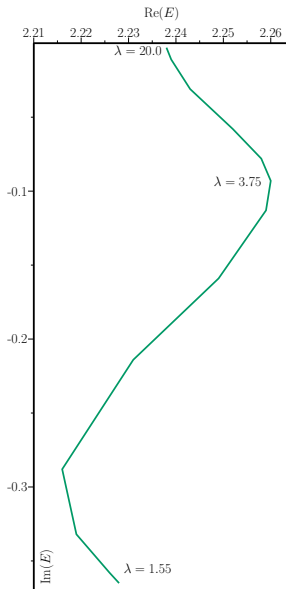


Figure: Confinement pole  $n=2$ , variation with  $\lambda$

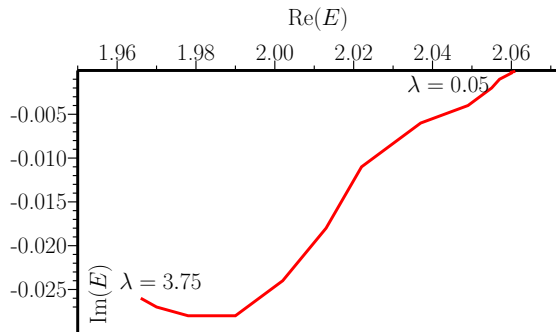
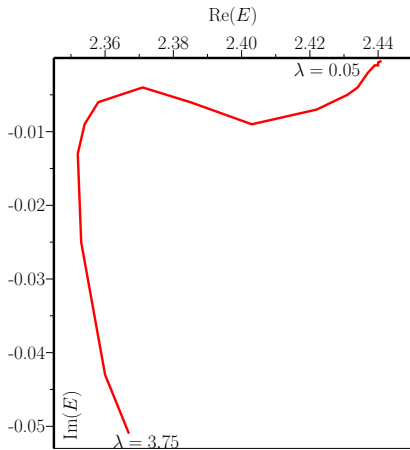


Figure: Confinement pole  $n=3$ , variation with  $\lambda$





Finally, we show some cross sections. The 1st figure shows the  $KK$  cross section from threshold upwards. We see the huge and narrow  $\phi(1020)$  peak as well as its first radial excitation. We interpret the latter state at about 1.5 GeV as the  $2^3S_1$  state and the  $\phi(1690)$  as the  $1^3D_1$  (not included here). The next radial excitation is not visible here, but it is in another channel ( $K^*K^*$ ).

The 2nd figure shows the  $f_0(980)\phi$  cross section above 2.0 GeV. Note that no sign of the continuum poles is visible. Note, however, that the  $X(2175)$  was observed in a production process and not in elastic scattering as described by us. Poles are universal, but cross sections are not.

Also the confinement pole at about  $2.37 - i0.05$  GeV leaves no trace, but it is clearly visible in the  $K^*K_1(1270)$  channel (see 3rd figure)

Figure: Cross Section for the  $KK$  channel

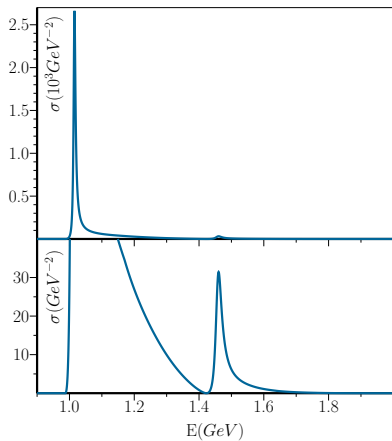


Figure: Cross Section for the  $f_0\phi$  channel

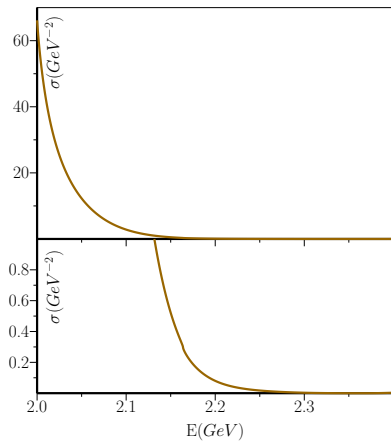
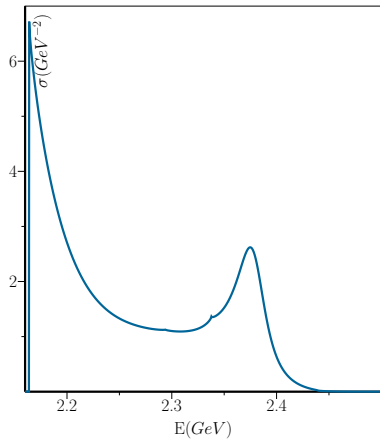


Figure: Cross Section for the  $K^* K_1(1270)$  channel



## IV. Conclusions and improvements

- ◇ Coupling several channels to bare  $s\bar{s}$  states produces dynamical poles. One of these may give rise to the  $X(2175)$  signal.
  - ◇ The coupled-channel effects are large and non-linear in the coupling.
  - ◇ Therefore, a more detailed investigation is needed for reliable predictions.
- 
- ▷ The  $^3D_1$  quark-antiquark states should be coupled as well.
  - ▷ We may consider deviations from ideal mixing.
  - ▷ Non-zero widths of decay products might be accounted for.
  - ▷ The transition potential might be made more realistic.